Model Synthesis and Identification of a Hodgkin-Huxley-Type GnRH Neuron Model

Dávid Csercsik, Gábor Szederkényi, Katalin M. Hangos and Imre Farkas

Abstract— **GnRH neurons are key elements of the reproductive neuroendocrine system and play important central regulating role in the dynamics of the hormonal cycle. A conductance-based Hodgkin-Huxley model structure is proposed in this paper in the form of nonlinear ordinary differential equations that is able to take into account up-to-date biological literature data related to ion channels. Measurement data were available for parameter estimation, which are originated from laboratory experiments done in the Institute of Experimental Medicine of the Hungarian Academy of Sciences in the form of whole cell patch-clamp recordings. The proposed neuron model is highly nonlinear in parameters and the evaluation of the objective function is computationally expensive, therefore the asynchronous parallel pattern search (APPS) procedure has been used for identification which is a gradient-free optimization method that can handle linear equality and inequality constraints and has advantageous convergence properties. The model with high number of estimated parameters provides a qualitatively good fit of both voltage clamp and current clamp traces.**

I. INTRODUCTION

Neurons are interesting dynamical systems where a combination of physico-chemical reactions and bio-physical (electrical) phenomena are taking place. Dynamical modeling and parameter estimation of neurons is a challenging and quickly developing area with great importance in understanding the operation of certain physiological processes and potential use in research, therapy and drug design [1]. Although there were numerous attempts for the identification of neuron models (see, e.g. [2]), the computational methods and techniques in systems biology are not so elaborate and well-analyzed than in more traditional engineering fields [3] (often due to the high degree of problem complexity).

A. The role of GnRH neurons in the female reproductive neuroendocrine system

The system of ovarian and pituitary hormones regulates and maintains the menstrual/hormonal cycle in adult women. During the menstrual cycle, the anterior pituitary, affected by gonadotropine-releasing hormone (GnRH) secreted in the hypothalamus, secretes hormones in a pulsatile way to stimulate the growth and development of ovarian follicles: follicle-stimulating hormone (FSH) and luteinizing hormone (LH). Consequently, cells in the ovaries secrete hormones which affect the secretion of GnRH and pituitary hormones: Estradiol (E_2), progesteron (P_4) and inhibin (Ih) [4].

Central control of reproduction in vertebrates is governed by a neuronal pulse generator that underlies the activity of hypothalamic neuroendocrine cells that secrete GnRH. Bursts and prolonged episodes of repetitive action potentials have been associated with hormone secretion in this and other neuroendocrine systems [5].

Majority of the GnRH pulse generator models that can be found in literature nowdays, use very simple neuron models and networks. Furthermore these models are neither based on the known membrane properties of GnRH neurons, nor are able to describe the effect of ovary hormones [6], [7].

Based on the above motivation, the main purpose of this work is to develop a method to estimate the parameters of a simple GnRH neuron model, based on laboratory measurements.

This work is intended to be the first step in a bottom-up procedure which aims to build a hierarchical model of the GnRH pulse generator that includes the effects of ovarial hormones.

II. THE GNRH NEURON

The pulsatile release of GnRH is driven by the intrinsic activity of GnRH neurons, which is characterized by bursts of action potentials correlated with oscillatory increases in intracellular [Ca^{2+}]. Several in vitro experiments have shown that changes in cytosolic Ca^{2+} concentration determine the secretory pattern of GnRH [8], suggesting that Ca^{2+} plays a central role in the signal transduction processes that lead to exocytosis. Furthermore, GnRH secretion from perifused GT-1 and hypothalamic cells is reduced by L-type Ca^{2+} channel inhibitors and augmented by activation of voltage-gated Ca^{2+} channels (VGCC) [9].

Furthermore, several results point to the fact that the membrane dynamics and hormone secretion of GnRH neurons is affected by peripherial hormones estradiol (E_2) [10], [11], [12], [13] and progesterone (P_4) [14], [15].

A. Basic membrane properties and ion channels of the GnRH neuron

Experiments of Bosama et al. showed that the GT-1 cell line expressed a tetrodotoxin (TTX)-sensitive Na channel, two types of Ca channels, three types of outward K channels and an inward rectifier K^+ channel [16].

This work was supported by the Hungarian Research Fund OTKA through grant K67625. Gábor Szederkényi is a grantee of the Bolyai scholarship of the Hungarian Academy of Sciences.

Dávid Csercsik, Gábor Szederkényi and Katalin M. Hangos are with the Process Control Research Group, Systems and Control Laboratory, Computer and Automation Research Institute, HAS, Budapest Hungary csercsik@scl.sztaki.hu, szeder@scl.sztaki.hu, hangos@scl.sztaki.hu

Imre Farkas is with the Department of Endocrine Neurobiology, Institute of Experimental Medicine, HAS, Budapest, Hungary farkas@koki.hu

ISBN 978-963-311-369-1

Kusano et al. identified an inward rectifier type current, a tetrodotoxin-sensitive Na^+ current (I_{Na}) and two major types of K^+ currents, a transient current (I_A), a delayed rectifier current (I_K) and low- and high-voltage activated Ca^{2+} currents in cultures of embryonic GnRH neurons [17].

Van Goor et al. revealed the presence of T-type and L-type Ca^{2+} channels [18].

The families of electrotonic potentials evoked in individual adult GnRH neurons in response to short (20-30 msec duration) and long (200 msec) duration intracellular current pulses were found to be heterogeneous [19]. The most striking difference was observed in response to 200 msec hyperpolarizing current pulses where four main profiles (types I-IV) were consistently observed.

Adult GnRH neurons were found to fire Na^+ dependent action potentials, because 0.5 μmol TTX abolished evoked action potentials in all cells tested.

Further investigations [19] point to the probability of presence of $I_{Q/H}$ (large current potassium-activated) I_A (rapidly inactivating) and I_K (delayed rectifier) potassium channels.

According to [20], GnRH neurons express a variety of sodium, type I_{IR} (inward rectifying), I_A, and $I_{Q/H}$ potassium. and type T and N Ca^{2+} channels.

Constantin et al. found that whole-cell recordings of voltage-gated outward K^+ currents in GT1-1 neurons revealed at least two different components of the current. These included a rapidly activating transient component and a more slowly activating, sustained component [21]. Furthermore, according to this article, GT1-1 cells also express inwardly rectifying K^+ currents ($I_{K(IR)}$) that were activated by hyperpolarization in the presence of elevated extracellular K^+. These results of this article also indicate that specific subtypes of K^+ channels in GT1-1 cells can have distinct roles in the amplitude modulation or frequency modulation of Ca^{2+} signaling.

Watanabe et al. showed in [22] that GT1-7 cells express R-, L-, N-, and T-type voltage-gated Ca^{2+} channels. The results suggest that R-type was a major current component, and the L-, N-, and T-types were minor ones. The characterization of these voltage gated Ca^{2+} currents is detailed in [23].

III. Materials and methods

Based on literature data about the ion channels of the GnRH neuron and properties of ion channels, a simple GnRH neuron-model can be developed and identified via further literature data, voltage clamp and current clamp measurements.

This basic membrane dynamics-model is considered to be acceptable, if it approximates available measurement data quantitatively well.

Thereafter, the model can be extended to take the effects of estradiol on the membrane currents and dynamics into account.

A. Measurement data

1) Obtaining and preparing samples: Mouse brain was used for obtaining GnRH neurons for measurements. The mouse was decapitated, and the brain was rapidly removed and placed in ice-cold artificial cerebrospinal fluid (ACSF) oxygenated with 95% O_2-5% CO_2 mixture. Brains were blocked and glued to the chilled stage of a vibratome, and 250-micrometer-thick coronal slices containing the medial septum through to the preoptic area were cut. The slices were then incubated at room temperature for 1 hour in oxygenated ACSF consisting of (in mM): 135 NaCl, 3.5 KCl, 26 $NaHCO_3$, 10 D-glucose, 1.25 NaH_2PO_4, 1.2 $MgSO_4$, 2.5 $CaCl_2$., pH 7.3.

2) Whole-cell recording of GnRH neurons: Slices were transferred to the recording chamber, held submerged, and continuously superfused with oxygenized ACSF. All recordings were made at 33°C.

In order to visualize GnRH neurons in the brain slices, GnRH-enhanced green fluorescent protein (GnRH-GFP) transgenic mice (kind gift by Dr. Suzanne Moenter) were chosen in which the GnRH promoter drives selective GFP expression in the majority of GnRH neurons. GnRH-GFP neurons were identified in the acute brain slices by their green fluorescence, typical fusiform shape and apparent topographic location in the preoptic area.

The electrodes were filled with intracellular solution (in mM): 140 KCl, 10 HEPES, 5 EGTA, 0.1 $CaCl_2$, 4 MgATP, 0.4 NaATP, pH 7.3 with NaOH. Resistance of patch electrodes was 2-3 MΩ. Holding potential was -70 mV, near the average resting potential of the GnRH cells. Pipette offset potential, series resistance and capacitance were compensated before recording.

The protocol for voltage clamp recordings was: twelve voltage steps were applied starting from the holding potential. The first step was -70mV and the subsequent steps were increased by 10 mV. Duration of the steps was 30 ms.

The protocol for current clamp recordings to activate action potentials (APs) was: the holding current was 0 pA. First the resting potential was measured then current step of 10 pA and 200 ms was applied to the cells. If the 10 pA current failed to evokeAPs, it was elevated by 10 pA steps till it induced 3-4 APs.

B. Model development

The suggested model framework of single cell models: A single compartment Hodgkin-Huxley (HH) type model [24] is suggested, which later can be extended to a multicompartmental structure. The main benefits of this model class are the following:

- Modularity: Each ion channel is represented by an element of the model (conductance), so different ion channels can be taken into account separately, and in a modular way. This structure allows the integration of the most available literature data into the model.
- The properties of specific ion channels can be measured separately via voltage clamp (reversal potential-based) methods, and pharmacological (TTX, TEA, etc. based) methods. These types of measurements can gather data corresponding to specific elements of the model. This implies the benefit of the opportunity, that various

elements of the model can be identified separately, using different parameter estimation methods, if needed.
- Because the different ion channels are described by different elements of the model, the model can be be extended with equations describing the effect of estradiol, acting on specific ion channels.

Elements of the model: According to the literature data detailed in II-A, previous results point to the existence of the following components on the level of conductance elements in the HH model:

- Na^+ channel: A simple voltage gated inward rectifier Na^+ channel can be assumed, with standard characteristics [16], [17]. The current related to this channel will be denoted by I_{Na1}.
- A voltage gated transient or rapidly activating/inactivating K^+ channel is also taken into account, responsible for the rapid, transient component of the outward K^+ current (I_{K1}) [17], [21], [19], [16], [20].
- A voltage gated delayed outward rectifier K^+ channel can be assumed, which contributes to the more slowly activating, sustained component of the outward K^+ current (I_{K2}) [17], [21], [19], [16], [20].
- Low voltage gated (T-type) Ca^{2+} channels, which are activated in earlier phases of depolarization (I_{Ca1}) [23], [18], [20].
- High voltage gated (L-type) Ca^{2+} channels (I_{Ca2}) [9], [18].
- Static leakage currents with constant conductance (I_L).

The **equivalent electric circuit** of a one-compartment GnRH neuron model in the case when all conductances are taken into account can be depicted as it is shown in fig. 1.

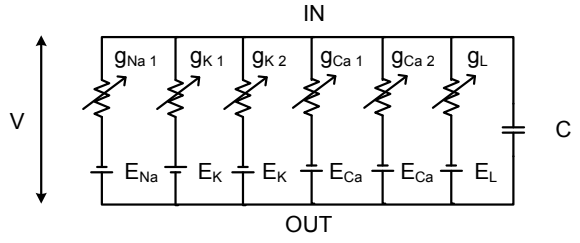

Fig. 1. Parallel conductance model, with conductances representing different ion channels

Literature data of qualitative features and parameters related to some of the above ion channels can be found in [25], [26], [23].

Model equations: The model depicted in fig. 1 can be described with the following equations:

$$\frac{dV}{dt} = -\frac{1}{C}(I_{Na1} + I_{K1} + I_{K2} + I_{Ca1} + I_{Ca2} + I_L) + \frac{1}{C}I_{ex}$$

$$\frac{dm_i}{dt} = (m_{i\infty} - m_i)/\tau_{mi} \qquad \frac{dh_i}{dt} = (h_{i\infty} - h_i)/\tau_{hi}$$

where V is the the membrane voltage, C is the membrane capacitance, I_{Na1} denotes the sodium current, I_{Ki} denotes the various potassium currents, I_{Cai} stands for the calcium currents, I_L for the leakage. The m_i and h_i variables are the activation and inactivation variables of the corresponding currents. $m_{i\infty}, h_{i\infty}$ and $\tau_{mi/hi}$ denote the steady-state activation and inactivation functions, and the voltage dependent time constants of activation and inactivation variables, which are nonlinear Boltzmann and Gauss -like functions of the membrane potential:

$$a_{\infty i} = \frac{1}{1 + e^{\frac{V_{half_{ai}} - V}{K_{ai}}}}$$

$$a \in \{m, h\} \qquad i \in \{1, 2, 3, 4, 5\} \qquad K_{mi} > 0, K_{hi} < 0 \quad \forall i$$

$$\tau_{ai} = C_{base_{ai}} + C_{amp_{ai}}\, e^{\frac{-(V_{max_{ai}} - V)^2}{\sigma_{ai}^2}}$$

Finally, I_{ex} refers to the external injected current, and the indices refer to: $i = 1$ - I_{Na1}, $i = 2$ - I_{K1}, $i = 3$ - I_{K2}, $i = 4$ - I_{Ca1}, $i = 5$ - I_{Ca2}. The currents of ionic channels are

$$I_{Na1} = \bar{g}_{Na1} m_1^3 h_1 (V - E_{Na}) \qquad I_{K1} = \bar{g}_{K1} m_2^4 h_2 (V - E_K)$$
$$I_{K2} = \bar{g}_{K2} m_3 h_3 (V - E_K) \qquad I_{Ca1} = \bar{g}_{Ca3} m_4 h_4 (V - E_{Ca})$$
$$I_{Ca2} = \bar{g}_{Ca2} m_5^2 h_5 (V - E_{Ca}) \qquad I_L = \bar{g}_L (V - E_L)$$

where the E_{Na}, E_K, E_{Ca} and E_L denote the reversal potentials of the corresponding ions and the leakage current.

C. Parameter estimation

1) Basic identification setup: The identification was based on both voltage clamp and current clamp measurements. In the case of voltage clamp, the term I_{ex} in the differential equation corresponding to the transmembrane voltage was modified: $I_{ex} = p(V_{clamp} - V)$. Considering this modification, with a p big enough, the desired voltage step could be simulated with the same model used later for current clamp simulations.

Voltage Clamp (VC): The manipulated external input to the system was the excitation voltage V_{clamp}. Three square signals of different amplitudes were used as inputs. The parameter of the voltage steps were the following: The holding potential was -70mV, and voltage steps of 40, 30 and 20 mV were applied from 10 to 40 ms. The measured output was the total output membrane current:

$$I_{out} = I_{Na1} + I_{K1} + I_{K2} + I_{Ca1} + I_{Ca2} + I_L$$

The objective function of the estimation was the standard two-norm of the difference between the measured and computed output currents for the three measurements, i.e.

$$W(\theta)_{VC} = \frac{1}{N}\|I^m_{out,1} - I^s_{out,1}\|_2 + \frac{1}{N}\|I^m_{out,2} - I^s_{out,2}\|_2 + \frac{1}{N}\|I^m_{out,3} - I^s_{out,3}\|_2 \qquad (1)$$

where θ is the estimated parameter vector, and $I^m_{out,i}$ and $I^s_{out,i}$ for $i = 1, 2, 3$ denote the measured and model computed (simulated) total output current (as a discrete time sequence) for the ith measurement, respectively. Furthermore, N is the number of data points. The sampling time of the VC measurements was 0.1 ms.

Current Clamp (CC): The manipulated external input to the system was the excitation current I_{ex}.

A square signal of 50 pA of amplitude was used as input, that was applied from 50 to 250 ms. The measured output was the membrane voltage V. The objective function takes the form:

$$W(\theta)_{CC} = \frac{1}{N}\|V^m_{out,1} - V^s_{out,1}\|_2$$

where the notations refer to the measured and estimated signals as in the case of VC.

The resulting value of the objective function can be calculated as:

$$W(\theta) = W(\theta)_{CC} + W(\theta)_{VC}$$

The sampling time of the CC measurements was 0.5 ms.

Before applying the optimization algorithm, intuitive rough-tuning of the activation parameters (parameters of the Boltzmann and Gauss functions) and conductance values was performed to capture some qualitative features of the neural behavior (e.g. the model should fire action potentials as response to the exciting current, the firing frequency, the local maxima after the appearance of the exciting current should be similar). This preparation proved to be necessary for convergence to an acceptable optimum. The intuitive initialization of activation parameters was based mainly on decomposition of the CC trace. The considered parts of the CC trace are shown in fig 4. This means that from different parts of the CC trace, the initial values of different parameters were guessed:

- *Resting potential*: determined by the leak, delayed rectifier (I_{K2}), Ca_1 conductances and steady-state parameters (m_∞, h_∞).
- *Injected current-induced depolarization* is altered by C and the K,Na,Ca currents
- *Upstroke of AP*is influenced by Na current
- *Downstroke of AP* is determined mainly by Na, K currents
- *Interspike intervals* are influenced by K_2, Ca, Leak currents

According to the estimated activation parameters, the maximal channel conductances were estimated from VC and CC data. After a result for conductance values, the activation parameters were further tuned via numerical optimization.

D. Optimization algorithm

Since the activation variables can not be measured, a simulation based minimization of the objective function was performed. Because of the model nonlinearity, the objective function value can be a complicated function of the estimated parameters. Moreover, the precise simulation of the system dynamics for a given parameter set is computationally quite demanding, i.e. a few hundred evaluations of the objective function takes a couple of hours on a typical desktop PC. This also means that avoiding the numerical approximation of the gradients of the objective function was desirable in our case.

The above facts motivated us to choose the freely available Asynchronous Parallel Pattern Search (APPS) algorithm for parameter estimation. Parallel pattern search (PPS) is a useful tool for derivative-free optimization where the number of variables is not large (about fifty or less) and the objective function is expensive to evaluate [27]. The basic PPS algorithm is very simple, its main steps are the following (where f denotes the objective function to be minimized):

Initialization:

- Set the iteration counter $k = 0$.
- Select a set of search directions $\mathcal{D} = \{d_1, \ldots, d_p\}$.
- Select a step-length control parameter Δ_0.
- Select a stopping tolerance tol.
- Select a starting point x_0 and evaluate $f(x_0)$.

Iteration:

1) Compute $x_k + \Delta_k d_i$ and evaluate $f(x_k + \Delta_k d_i)$, for $i = 1, \ldots, p$ concurrently.
2) Determine x_+ and $f(x_+)$ such that $f(x_+) = \min\{f(x_k + \Delta_k d_i), i = 1, \ldots, p\}$.
3) If $f(x_+) < f(x_k)$, then $x_k \leftarrow x_+$ and $f(x_k) \leftarrow f(x_+)$. Else $\Delta_k \leftarrow \frac{1}{2}\Delta_k$.
4) If $\Delta_k > tol$, $k \leftarrow k + 1$, go to Step 1. Else, exit.

The APPS algorithm is an asynchronous extension of the PPS method that efficiently handles situations when the individual objective function evaluations may take significantly different time intervals and therefore it is very suitable to be implemented in a parallel or grid environment. Furthermore, recent implementations of the APPS method handle bound and linear constraints on the parameters [28]. The global convergence of APPS under standard assumptions is also proved [29]. These advantageous properties suggest that APPS can be a good choice to solve simulation-intensive optimization problems.

IV. Results and Discussion

As a result of the initializing and the algorithm a parameter set was found, which provided good approximation of several qualitative features (eg. firing only during current injected, resting potential).

It has to be noted that the simulations were started from the initial voltage corresponding to the observed resting potential, and all activation values were set to their steady-state values, corresponding to this voltage.

Furthermore, the simulation with the resulting parameters reproduced even some of critical elements (eg. the local maxima of the voltage trace before the AP in the CC).

Regarding activation parameters, only 5 of them had to be changed drastically (belonging to fast Na and K currents to speed up the downstroke of action potentials, and influence the maxima of the voltage clamp traces). The initialization of parameters suggested that without these modifications the action potentials are qualitatively different from the observed ones.

The measured and simulated results of the voltage clamp measurements with the two highest voltage step are depicted in figure 2 and 3.

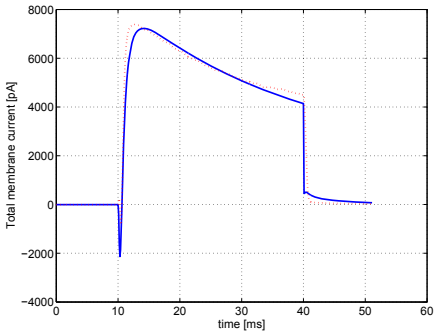

Fig. 2. Measured and simulated membrane currents in the case of VC: Dotted line - measured, continual - simulated

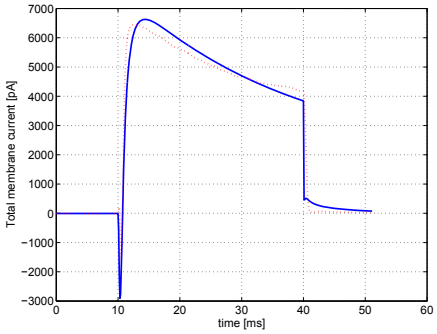

Fig. 3. Measured and simulated membrane currents in the case of VC Dotted line - measured, continual - simulated

The measured and simulated results of current clamp measurements are depicted in figure 4.

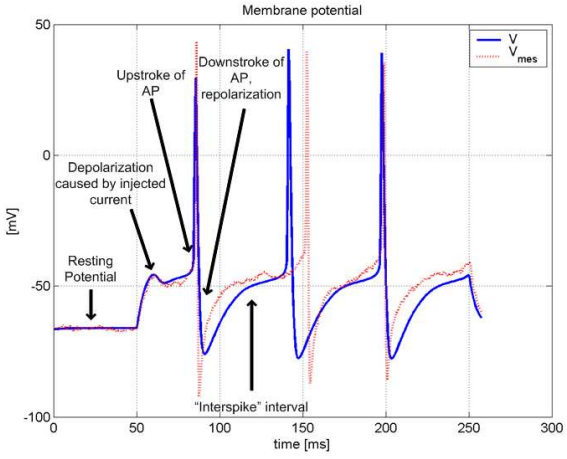

Fig. 4. Measured and simulated membrane voltage in the case of CC

The conductance values and currents during simulation are depicted in figures 5 and 6. In these figures it can be seen that according to simulation results, the action potential upstroke is dominantly determined by the sodium current, while the T-type Ca current plays a role in the depolarization in the interspike intervals. The figure also shows that the local maxima at the beginning of the voltage trace (4) can be related to the fast potassium current. This can be questionable from the physiological point of view, because this type of potassium current is usually observed only after strong hyperpolarization (or prepulse). Figures 5 and 6 furthermore suggest that the fast and the delayed rectifier potassium currents determine the downstroke of action potentials together, and the delayed rectifier current plays also significant role in the interspike intervals, affecting the firing frequency.

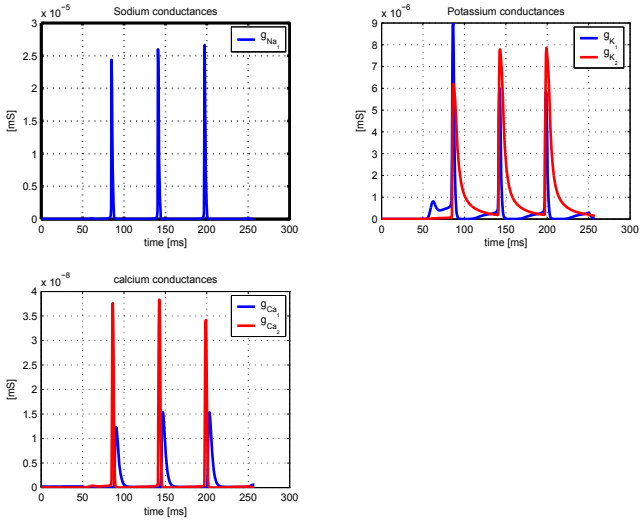

Fig. 5. Conductances in the simulated model

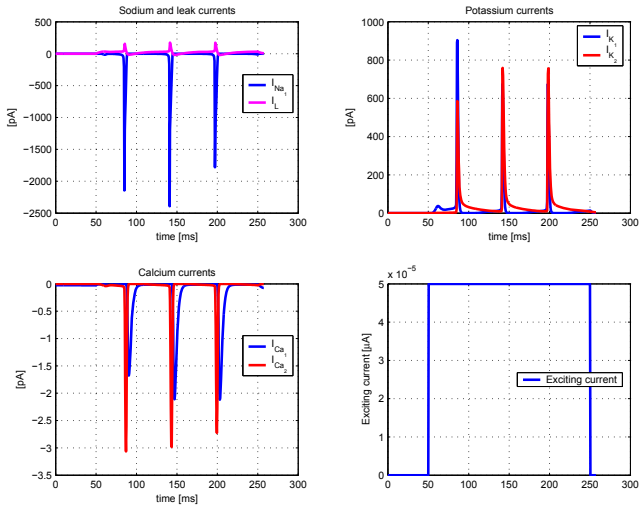

Fig. 6. Currents in the simulated model

In contrast to the above promising results, the actual parametrization (which includes low Ca conductance values) implies very low amplitude Ca currents, which results are physiologically questionable. This suggests that search for possible other parameter sets, and measurements with channel blockers or Ca imaging is required.

Furthermore the simulations suggest, that the local maxima of the voltage trace at the beginning of the depolarization due to the injected current, can be mainly connected to the appearance of the fast potassium current. This is in contradiction with the observations made in the case of this type of neurons, which claim that this type of current can only be observed after strong repolarization, which is necessary to de-inactivate the potassium current [12].

In addition, excitability properties are not fully reproduced by the simulations done with the resulting parameters: It is expected that the model should not fire at all at smaller injected current but the simulations showed that in the case of a 40 pA exciting current, the model still fires action potentials, but with significant lower frequency.

V. Conclusions and future work

In this article a Hodgkin-Huxley type model of the GnRH neuron was suggested, based on biological literature data. Based on voltage clamp and current clamp measurements, the asynchronous parallel pattern search (APPS) procedure was used for parameter identification. The model with the estimated parameters provides a qualitatively good fit of voltage clamp and current clamp traces, although the high number of parameters had to be tuned to reach the appropriate behavior. This suggest that the model is possibly overparametrized. The resulting parameter set showed great sensitivity to the initial conditions of the optimization, which were tuned intuitively.

Future work will be directed towards analyzing the identifiability of the model, and finding the parameter set which is unique and optimal. Further experiments are also planned using channel blockers.

VI. Acknowledgments

The authors gratefully acknowledge the Laboratory of the Department of Endocrine Neurobiology at the Institute of Experimental Medicine for the opportunity of access to patch clamp measurement data.

References

[1] E. Izhikevich, *Dynamical Systems in Neuroscience*. 999 Riverview Drive Suite 208 Totowa New Jersey 07512: The MIT Press, 2005.

[2] J. Tien and J. Guckenheimer, "Parameter estimation for bursting neural models," *Journal of Computional Neuroscience*, vol. 24, pp. 358–373, 2008.

[3] P. Dhurjati and R. Mahadevan, "Systems biology: the synergetic interplay between biology and mathematics," *The Canadian Journal of Engineering*, vol. 86, p. 141, 2008.

[4] P. Conn and M. Freeman, *Neuroendocrinology in Physiology and Medicine*. 999 Riverview Drive Suite 208 Totowa New Jersey 07512: Humana Press, 2000.

[5] R. Wilson, J. Kesner, J. Kaufmann, T. Uemura, T. Akema, and E. Knobil, "Central electrtophsysiological correlates of pulsatile lutenizing hormone secretion in the rhesus monkey," *Neuroendocrinology*, vol. 39, pp. 256–260, 1984.

[6] D. Brown, A. Herbison, J. Robinson, R. Marrs, and G. Leng, "Modelling the lutenizing hormone-releasing hormone pulse generator," *Neuroscience*, vol. 63, pp. 869–879, 1994.

[7] J. Gordan, B. Attardi, and D. Pfaff, "Mathematical exploration of pulsatility in cultured gonadotropin-releasing hormone neurons," *Neuroendocrinology*, vol. 67, pp. 2–17, 1998.

[8] S. Stojilkovic, L. Krsmanovic, D. Spergel, and K. Catt, "GnRH neurons: intrinsic pulsatility and receptor-mediated regulation." *Trends in Endocrinology and Metabolism*, vol. 5, pp. 201–209, 1994.

[9] L. Krsmanovic, S. Stojilkovic, F. Merelli, S. Dufour, M. Virmani, and K. Catt, "Calcium signaling and episodic secretion of gonadotropin-releasing hormone in hypothalamic neurons," *Proceedings of the National Academy of Sciences of the USA*, vol. 89, pp. 8462–8466, 1992.

[10] R. DeFazio and S. Moenter, "Estradiol feedback alters potassium currents and firing properties of gonadotropin- releasing hormone neurons," *Molecular Endocrinology*, vol. 16, pp. 2255–2265, 2002.

[11] R. Maurer, K. Kim, W. Schoderbek, M. Robertson, and D. Glenn, "Regulation of glycoprotein hormone alpha-subunit gene expression," *Recent Progress in Hormone Research*, vol. 129, pp. 1175–82, 1999.

[12] I. Farkas, P. Varju, and Z. Liposits, "Estrogen modulates potassium currents and expression of the Kv4.2 subunit in GT1-7 cells," *Neurochemistry International*, vol. 50, pp. 619–627, 2007.

[13] A. Herbison, "Estrogen positive feedback to gonadotropin-releasing hormone (GnRH) neurons in the rodent: The case for the rostral periventricular area of the third ventricle (RP3V)," *Brain Research Reviews*, vol. doi:10.1016/j.brainresrev.2007.05.006, 2007.

[14] F. Karsch, J. Cummins, G. Thomas, and I. Clarke, "Steroid feedback inhibition of pulsatile secretion of gonadotropin-releasing hormone in the ewe," *Biology of Reproduction*, vol. 36, pp. 1207–18, 1987.

[15] N. Chabbert-Buffet, D. Skinnerb, A. Caratyb, and P. Boucharda, "Neuroendocrine effects of progesterone," *Steroids*, vol. 65, pp. 613–620, 2000.

[16] M. Bosama, "Ion channel properties and episodic activity in isolated immortalized gonadotropin-releasing hormone (GnRH) neurons," *Journal of Membrane Biology*, vol. 136, pp. 85–96, 1993.

[17] K. Kusano, S. Fueshko, H. Gainer, and S. Wray, "Electrical and synaptic properties of embryonic lutenizing hormone-releasing hormone neurons in explant cultures," *Proceedings of the National Academy of Sciences of the USA*, vol. 92, pp. 3918–3992, 1995.

[18] F. Van Goor, L. Krsmanovic, K. Catt, and S. Stojilkovic, "Control of action potential-driven calcium influx in gt1 neurons by the activation status of sodium and calcium channels," *Molecular Endocrinology*, vol. 13, pp. 587–603, 1999.

[19] J. Sim, M. Skynner, and A. Herbison, "Heterogeneity in the basic membrane properties of postnatal gonadotropin-releasing hormone neurons in the mouse," *The Journal of Neuroscience*, vol. 21, pp. 1067–1075, 2001.

[20] A. Herbison, J. Pape, S. Simonian, M. Skynner, and J. Sim, "Molecular and cellular properties of GnRH neurons revealed through transgenics in mouse," *Molecular and Cellular Endocrinology*, vol. 185, pp. 185–194, 2001.

[21] J. Constantin and A. Charles, "Modulation of Ca^{2+} signaling by K^+ channels in a hypothalamic neuronal cell line (GT-1)," *Journal of Neurophysiology*, vol. 85, pp. 295–304, 2001.

[22] M. Watanabe, Y. Sakuma, and M. Kato, "High expression of the R-type voltage-gated Ca^{2+} channel and its involvement in Ca^{2+}-dependent gonadotropin-releasing hormone release in GT1-7 cells," *Endocrinology*, vol. 145, pp. 2375–2388, 2004.

[23] M. Kato, K. Ui-Tei, M. Watanabe, and Y. Sakuma, "Characterization of voltage-gated calcium currents in gonadotropin-releasing hormone neurons tagged with green fluorescent protein in rats," *Endocrinology*, vol. 144, pp. 5118–5125, 2003.

[24] A. Hodgkin and A. Huxley, "A quantitive description of membrane current and application to conduction and excitation in nerve," *Journal of Physiology*, vol. 117, pp. 500–544, 1952.

[25] H. Rehm and B. Tempel, "Voltage-gated k^+ channels of the mammalian brain," *FASEB J.*, vol. 5, pp. 164–170, 1991.

[26] K. Talavera and B. Nilius, "Biophysics and structure-function relationship of T-type Ca^{2+} channels," *Cell Calcium*, vol. 40, pp. 97–114, 2006.

[27] P. D. Hough, T. G. Kolda, and V. J. Torczon, "Asynchronous parallel pattern search for nonlinear optimization," *SIAM Journal on Scientific Computing*, vol. 23, pp. 134–156, 2000.

[28] T. G. Kolda, "Revisiting asynchronous parallel pattern search for nonlinear optimization," *SIAM J. Optim.*, vol. 16, pp. 563–586, 2005.

[29] T. Kolda and V. Torczon, "On the convergence of asynchronous parallel pattern search," *SIAM J. Optim.*, vol. 14, pp. 939–964, 2004.